Spheroid mechanics and implications for cell invasion

Boot, Ruben C.; Koenderink, Gijsje H.; Boukany, Pouyan E.

DOI
10.1080/23746149.2021.1978316

Publication date
2021

Document Version
Final published version

Published in
Advances in Physics: X

Advances in Physics: X

ISSN: (Print) (Online) Journal homepage: https://www.tandfonline.com/loi/tapx20

Spheroid mechanics and implications for cell invasion

Ruben C. Boot, Gijsje H. Koenderink & Pouyan E. Boukany

To cite this article: Ruben C. Boot, Gijsje H. Koenderink & Pouyan E. Boukany (2021) Spheroid mechanics and implications for cell invasion, Advances in Physics: X, 6:1, 1978316, DOI: 10.1080/23746149.2021.1978316

To link to this article: https://doi.org/10.1080/23746149.2021.1978316

Published online: 23 Sep 2021.

ADVANCES IN PHYSICS: X
2021, VOL. 6, NO. 1, 1978316
https://doi.org/10.1080/23746149.2021.1978316

Taylor & Francis
Taylor & Francis Group

REVIEWS

OPEN ACCESS Check for updates

Spheroid mechanics and implications for cell invasion

Ruben C. Boot[a], Gijsje H. Koenderink[b] and Pouyan E. Boukany[a]

[a]Department of Chemical Engineering, Delft University of Technology, Delft, The Netherlands; [b]Department of Bionanoscience, Kavli Institute of Nanoscience Delft, Delft University of Technology, Delft, The Netherlands

ABSTRACT

Spheroids are widely used *in vitro* 3D multicellular model systems that mimic complex physiological microenvironments of tissues. As different cell types vary in deformability and adhesion, the choice of (heterogeneous) cell composition will define overall spheroid mechanics, including their viscoelasticity and effective surface tension. These mechanical parameters directly influence cell sorting and possibly cell invasion into the extracellular matrix. Spheroid models therefore provide fundamental insights in the relation between cellular mechanics and important physiological processes, such as tissue formation, embryonic tissue remodeling, and cancer metastasis. In this review, we first summarize and compare current biophysical tools that probe mechanics of spheroids either from the outside or from within, then relate spheroid mechanics to cell mechanics and cell-cell adhesion, and subsequently discuss the role of spheroid mechanics alongside surrounding microenvironment parameters in (cancer) cell migration. We conclude by pointing out the research gaps and drawing the attention to novel techniques that could shed more light on the biophysical characterization of spheroids in the framework of tissue remodeling and cancer metastasis.

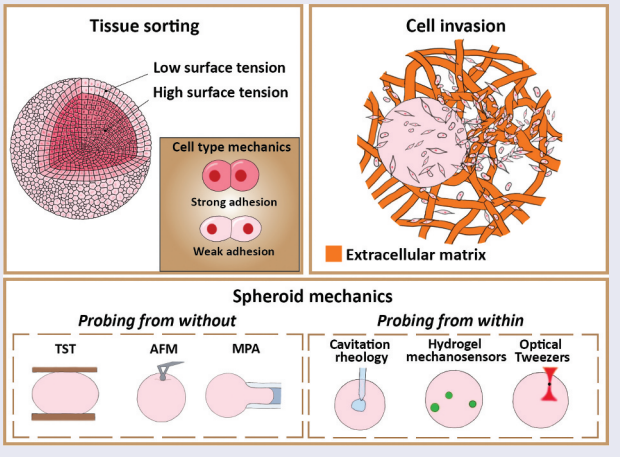

ARTICLE HISTORY
Received 1 July 2021
Accepted 2 September 2021

KEYWORDS
Cell sorting; cell invasion; tissue mechanics; mechanobiology; surface tension; active matter

CONTACT Pouyan E. Boukany p.e.boukany@tudelft.nl Department of Chemical Engineering, Delft University of Technology, van der Maasweg 9, 2629 HZ Delft, The Netherlands.

1 Introduction

The cells in our body routinely encounter a wide range of physical cues both from intra-cellular forces generated by molecular activity and from external mechanical forces [1]. Cells actively transduce these physical cues into biochemical signals that affect cell morphology, motility, arrangement and function in tissues [2–4]. The mechanical response of cells to forces and other physical cues such as confinement are therefore critical in the regulation of many physiological processes, such as cell division, growth and differentiation [2,5,6], tissue remodeling [7], wound-healing [8] and morphogenesis [9], and also in pathological processes like cancer cell invasion [10,11]. These processes rely heavily on the precise self-organization and mechanics of cellular systems in space and time. Furthermore, deviations from normal mechanical characteristics are directly correlated with the onset and progression of diseases such as cancer cell metastasis, inflammation and abnormal wound repair [12].

The mechanical response of multicellular tissues arises from the properties of the individual cells, alongside the interplay between these cells across multiple length scales [13]. While single cell mechanics are determined by the biophysical properties of their cytoskeleton and plasma membrane, the mechanical properties of tissues as a collective whole are determined by the complex linkage between cell adhesion molecules, the cytoskeleton and the extracellular environment [14,15]. In order to unravel this complexity, we therefore require techniques that allow us to probe tissue mechanics on different length scales, from the nanoscale to the macroscopic tissue scale.

To probe the mechanical properties of tissues and their responses to physical forces, suitable *in vitro* models that replicate both the multicellular nature and three-dimensional (3D) micro-environment found *in vivo* are required [16,17]. Nowadays, 3D multicellular systems such as spheroids and organoids have become appealing *in vitro* models to mimic complex physiological microenvironments of tissues. While spheroids are 3D spherical aggregates made from immortalized cell lines or primary cells, organoids arise from embryonic stem cells, induced pluripotent stem cells, or adult stem cells [18]. Organoid models represent the personalized *in vivo* environment more accurately than spheroids, but their generation requires a more complicated process, and is more time-consuming than spheroid production. As such, spheroids have become the most widespread 3D systems for basic biophysical characterization and are the focus in this review paper. Mechanical forces are integral to spheroid development and self-organization by regulating and changing their overall shape, cell packing density and internal cell arrangement. For instance, the interplay between various physical parameters (such as cell-cell adhesion, cortical

tension evoked by the cell's actomyosin cortex, and elasticity) strongly regulates cell sorting in embryos as shown in both 3D aggregates [19,20] and organoids [21–24]. Spheroids therefore allow us to probe a wide range of key biophysical parameters that influence tissue formation, tumour growth and cell invasion under relevant physical forces (such as shear stress) and gradients of biochemical cues (such as transforming growth factors and nutrients).

Often, tissues subjected to a force demonstrate viscoelastic behavior, with an elastic response at short-time scales and a viscous-like response at long-time scales [25]. When a mechanical load is applied, spheroids alter their shape and microstructure and consequently their mechanical response. This time-dependent behavior and responsiveness is reminiscent of that found in many glassy and colloidal systems in the field of soft condensed matter [26–30]. Thus, tissue biomechanics has become an appealing field for physicists to apply soft matter principles coupled with biophysical tools. These tools allow us to create a unified conceptual framework and unravel how mechanical forces deform cells in order to create functional healthy tissues and organs, heal wounds or induce pathological conditions such as cancer cell invasion [17,31–35].

While there are excellent reviews on spheroid formation [36], the role of physical principles in tissue formation [16,37], jamming transitions (in cancer and morphogenesis) [30,31] and probing of mechanical stress in living systems [38], a concise review on all the experimental tools for quantification of spheroid mechanics and how these tools have started to reveal mechanisms that govern spheroid mechanics and its implications for cell detachment and migration away from the spheroid is still missing. The main aim of this review is to close this gap by discussing the available state-of-the-art tools (Table 1), the relation between spheroid mechanics and tissue sorting, and implications for cell invasion. In the first half, the physiological relevance of spheroids as a 3D *in vitro* model is explained, followed by a discussion on available techniques for the biomechanical characterization of spheroids both from without and within. The second half of this review focuses on the self-organization of tissues and spheroids alongside present theoretical models explaining this phenomenon, focusing on the role of cellular adhesion, cortical tension and their coaction. Spheroid self-organization is subsequently linked to cell invasion in *in vitro* cancer metastasis models, and the influence of experimental parameters like interstitial fluid flows and surrounding extracellular matrix (ECM) type and density is discussed. Finally, the review concludes with a perspective on opportunities for future research. As the biophysics and soft matter communities gain insights into the fundamental mechanical properties of

Table 1. Techniques to analyse spheroid mechanics from without and within.

Spheroid analysis			
Technique	Analyzed parameter	Description	Source
Probing from without			
Atomic force microscopy (AFM)	Elastic modulus and viscoelasticity	Measuring cantilever deflection when indenting tissue.	[15,83,88,90,91,174]
Microtweezers	Elastic modulus	Tracking cantilever bending from customized replaceable cantilevers to determine applied force and tissue stiffness.	[92]
Micropipette aspiration (MPA)	Surface tension, elastic modulus and viscosity	Aspirating spheroid into micron-sized pipette and tracking the displacement of the front of the tongue with respect to the pipette tip over time.	[97,98,175]
Spheroid fusion	Bulk tissue fluidity	Analyzing coalescence of spheroids for a suitable amount of time (days).	[25,65,66,75,76]
Tissue surface tensiometry (TST)	Surface tension and viscosity	Analyzing relaxation force and shape relaxation after squeezing spheroid between parallel plates.	[20,25,63–65,78,79,176]
Probing from within			
Cellular scale			
Cavitation rheology	Tissue interfacial tension and elastic modulus	Analyzing pressure-growth relation for a spherical cavity induced in the material with a needle.	[50,105,177]
Hydrogel mechanosensors	Spatial distribution of mechanical stress in tissue	Defining the strain (change in volume) of incorporated hydrogel probes, allowing highly localized measurements of traction forces or mechanical pressure.	[112,113]
Subcellular scale			
Optical tweezers	Cytoplasmic stiffness	Measuring force-displacement relationship of unidirectionally dragged particles that are endocytosed by constituent cells.	[124]

spheroids and what distinguishes multicellular tumour spheroids from healthy cellular aggregates, important biophysical pathways and biomarkers for novel cancer therapeutics can be identified. Moreover, a fundamental understanding of the interplay of individual cell mechanics and cell-cell-interactions in overall tissue mechanics is essential when trying to understand tissue formation, or when designing strategies for tissue regeneration.

2 Mechanics of 3D multicellular spheroids

2.1 The physiological relevance of 3D *in vitro* spheroids

3D cell culture systems influence cell structure and mechanotransduction in a very different manner compared to traditional 2D monolayer culture set-ups [39]. Many cell types grown on 2D planar substrates become flatter, proliferate at an unnaturally rapid pace and lose their differentiated phenotype in comparison to their *in vivo* counterpart [40,41]. However, cells

regain their physiological form and function when reintroduced in a 3D environment. 3D cellular spheroids are an excellent *in vitro* model for tissues due to their physiologically relevant structure giving them several advantages. Firstly, their mechanical properties can be measured over both intracellular and intercellular length scales. Secondly, spheroids can be grown from a single cell line, allowing the reproduction of experiments on identical and reproducible replicates. Thirdly, cell growth and the biochemical environment, which alter mechanical properties of cells and tissues, can be meticulously controlled [42–44]. Due to the 3D nature of spheroids, cells in the core of the spheroid will receive less oxygen and nutrients and experience a lower pH than the outer cells, similar to *in vivo* tumours (Figure 1). When the inner cells are situated beyond the diffusion limit of approximately 200 μm from the edge of the spheroid, cell apoptosis occurs [45,46]. This results in the formation of a necrotic core surrounded by quiescent cells and an outer proliferating layer [47]. *In vivo*, tissue cells are located no further than 100 to 200 μm from the nearest capillary due to the limited diffusion of oxygen [48]. Cancer cells are capable of signalling for the formation of new blood vessels to overcome this fundamental limitation. This process creates a disorganised vasculature with an ineffective delivery of oxygen and nutrients to the tumour, resulting in similar concentration gradients as for *in vitro* spheroids [47].

Many techniques exist for generating spheroids (Figure 2). These include the hanging drop technique [49], liquid overlay [44,50], a shaking method that folds cell sheets into spheroids [51], droplet-based microfluidics [52,53], and many others. Importantly, spheroids can either be grown using a scaffold or by suspending cells in medium surrounded by non-adhesive walls. When using a scaffold, cells anchor to a 3D platform that mimics the extracellular matrix (ECM), which can be either natural (e.g. collagen), semi-synthetic (e.g. chitosan) or fully synthetic (e.g. polycaprolactone) [42]. For non-scaffold suspension-based techniques, cells float towards each other in suspension due to gravity after which they aggregate. Here, ECM is still present inside the spheroid due to proteins excreted by cells during the growth of the aggregate [54]. For a more extensive overview of the available spheroid culturing techniques and methodologies to analyse characteristics like size, growth and protein expression, the reader is referred to other reviews [36,42,55].

Importantly, the choice between a scaffold- or non-scaffold-based technique will define the polarity of cells at the tumour spheroid surface [56–58]. Cellular architecture and function are fundamentally dependent on this cell polarity, also termed apical-basal properties [59]. Epithelial cells that line the exterior and interior surfaces of our bodies form functionally distinct domains, termed apical and basal, and polarize along an apical-basal axis in order to form selectively permeable barriers (Figure 3(a)) [60]. The apical

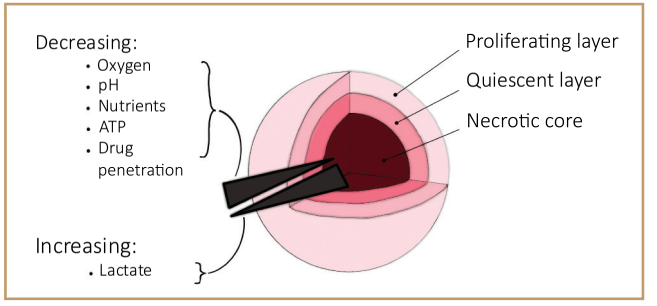

Figure 1. Spatial structure of a spheroid. Schematic of a spheroid demonstrating a necrotic core surrounded by quiescent cells and an outer proliferative layer, with a decreasing gradient of among others oxygen and pH towards the core, and an increasing gradient of lactate.

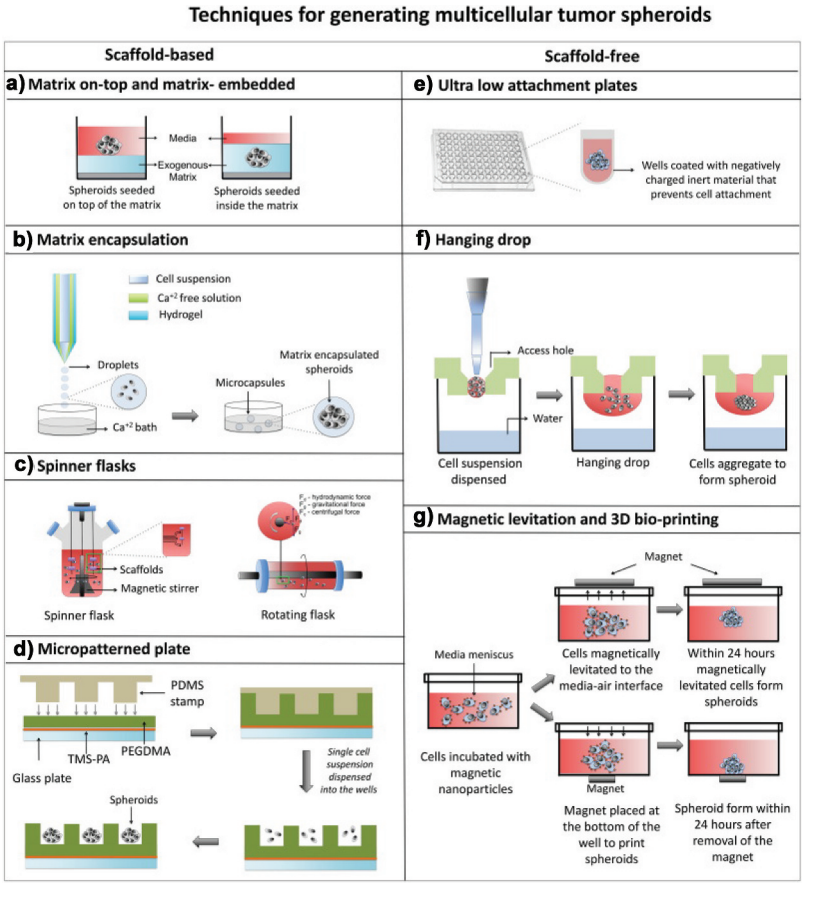

Figure 2. Spheroid growing techniques. Sorted into scaffold based (A-D) and scaffold-free techniques (E-G). Reprinted from [36], Copyright 2016, with permission from Elsevier.

side of the cell lines the lumen, hollow spaces in some of our major organs, and constitutes an exchange interface with other parts of the body. The basal side faces the basement membrane, the specialized cell surface-associated ECM on which cells live [61]. *In vivo*, the apical-basal polarity can differ between healthy and malignant tissues. For example, the invasive metastatic cancer spheroids found in the peritoneal cavity of colon cancer patients display a clear apical-out topology that is inverted compared to normal epithelial tissues [62]. *In vitro*, spheroids grown in a type I collagen-scaffold display an apical-in topology while spheroids in suspension have an apical-out architecture on their surface (Figure 3(b)) [56]. As such, the spheroid culturing technique should be carefully selected depending on the relevant *in vivo* tumour model.

2.2 Probing spheroids from without

2.2.1 Surface tension and viscosity

Just like *in vivo* embryonic tissues, heterogeneous spheroids composed of different cell lines are able to display spontaneous tissue segregation [63,64]. Similar to how one immiscible liquid tends to envelop another due to their difference in surface tensions, one cell line can envelop the other in a binary-mixed spheroid depending on cellular properties [65]. Understanding the physical mechanisms of cell sorting is important both at a fundamental level and at a more practical level in for example the field of 3D tissue bioprinting [66]. In the 1960s, the differential adhesion hypothesis (DAH) was formulated to explain this liquid-like phenomenon, and focused on the concept of tissue surface tension [67–69]. The model states that the rearrangement of cells is guided by the lowering of a cell population's adhesive-free energy as the amount of cell-cell bonding increases. As such, the mutual spreading mechanisms of tissues are specified by their relative surface tensions, which depend on the difference in intercellular adhesion of the different cell types [70,71]. For a pair of adhesive tissues, the tissue of lower surface tension will envelop the tissue with a higher surface tension [72]. This outcome has proven to be independent of the types of adhesion molecules utilized by the interacting cells [73]. The most widely studied classes of cell-cell adhesion receptors are the cadherins [74]. Spheroids have a surface tension that is a direct and linear function of their cadherin expression level [70]. Thus, a spheroid made out of two cell lines will rearrange in such a way that the cell line with a lower cadherin expression level spreads over the other [73]. Nowadays, there are however more sophisticated models that demonstrate regimes where the DAH breaks down. These will be introduced later on in this review.

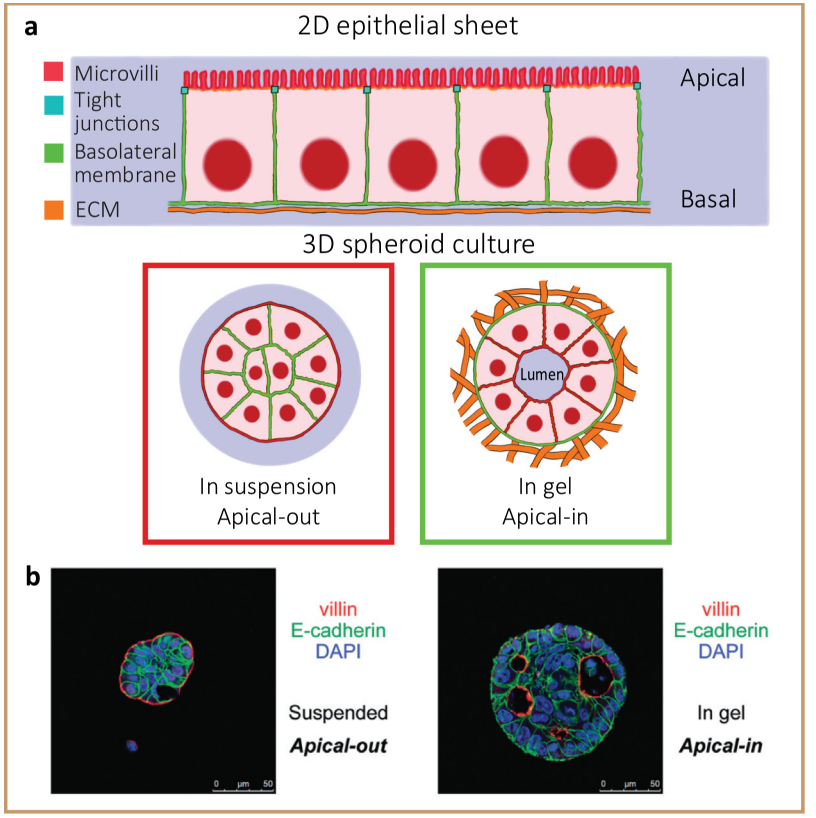

Figure 3. Cell polarity in multicellular assemblies. a) Schematic of apical-basal cell polarity in a 2D epithelial sheet where the basal side faces the ECM, and of spheroids, whose polarity depends on culturing technique. b) Immunofluorescence staining of colorectal cancer spheroids both in suspension and embedded in type I collagen cultured for 48 hours, demonstrating apical-out polarity when in suspension or apical-in when in a scaffold. Red: villin; green: E-cadherin; blue: DAPI. (b) is reprinted and adapted from [56], Copyright 2016, with permission from Elsevier.

Perhaps the most straightforward technique to get an indication of relative mechanics between cellular aggregates is **spheroid fusion** [75,76]. For this technique, two spheroids are brought together and allowed to fuse over time to give an indication of cell motility, also termed bulk tissue fluidity, and surface tension (Figure 4(a)) [25,65]. Making an analogy between spheroid fusion and the fusion of liquid droplets, the main parameters that define the fusion process are surface tension and viscosity. According to the liquid drop fusion model, higher surface tensions should result in shorter fusion times [77]. However, discrepancies to this model were found when epithelial spheroids with lower apparent surface tension fused faster than mesenchymal spheroids with higher surface tension [75]. This was most likely caused by processes such as extracellular matrix remodeling and dense cell packing in the mesenchymal spheroids. Nevertheless, the technique remains useful as measuring the fusion time gives an indication of how fluid-like or solid-like tissues are. Additionally, the cell and nucleus shapes during fusion give an indication of tissue fluidity and bulk mechanical behavior [76]. In samples from cancer patients, the degree of tissue fluidity is correlated with elongated cell and nucleus shapes, which in turn are linked to a higher motility. Cell and nucleus shape may thus identify metastatic potential during therapeutic treatment.

A widely used method to measure tissue surface tension is **tissue surface tensiometry (TST)**, also known as parallel plate tensiometry [63,64,78,79]. Here, a spherical aggregate is placed between two parallel compression plates (Figure 4(b)). Through continuous recording of both the force used to compress the spheroid and its contact angle with the plates, an apparent tissue surface tension is determined using the Laplace equation originally developed for simple liquids [78,79]. Only when successive compressions at different forces yield a similar surface tension, the spheroid can be considered liquid-like with an actual surface tension. This typically holds as long as spheroids are spherical and cells do not become fixed in position over time, for instance due to possible extracellular matrix build-up [63,64]. Of course, the assumption that spheroids are similar to liquid droplets is a clear oversimplification. Aggregates of cancer cells for instance often do not round up into spheroids and they often have a rough surface. Nevertheless, measuring the apparent tissue surface tension holds biological relevance when trying to explain observed tissue configurations and cell sorting.

2.2.2 Stiffness and elasticity

It has long been known that cells and tissues can display both solid-like elastic and fluid-like viscous behavior, making them viscoelastic [25]. Techniques that are able to measure this viscoelastic behavior both at a single-cell and tissue-level are of interest for several reasons. Firstly,

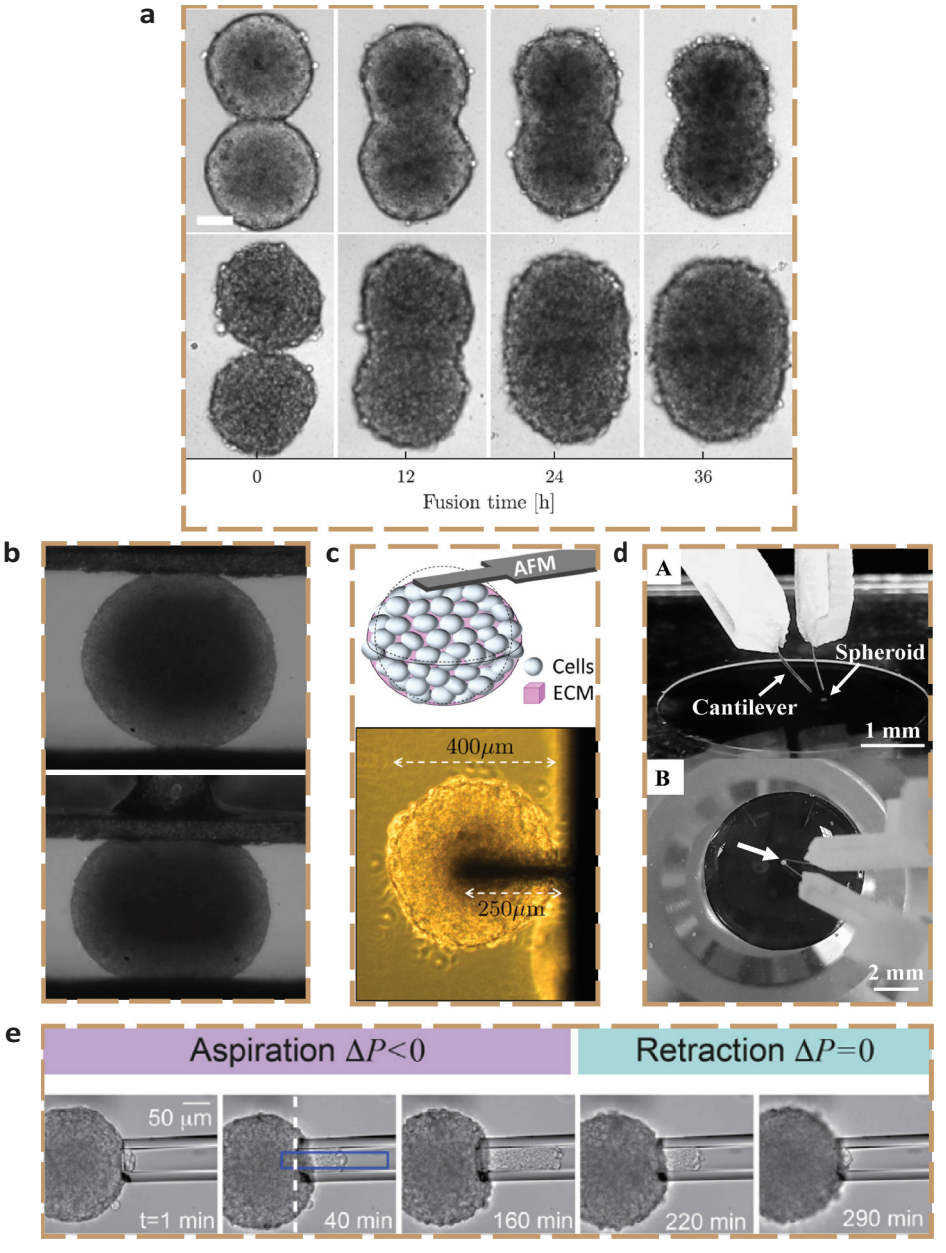

Figure 4. Probing spheroids from without. a) **Spheroid fusion** time series demonstrating cell type dependence. Spheroids formed from the non-tumourigenic MCF-10A cell line (top) fuse slower than spheroids made from metastatic MDA-MB-231 cells (bottom). Scale bar: 100 μm. b) **Tissue surface tensiometry** with an uncompressed (top) and compressed (bottom) spheroid in culture medium. c) Schematic and image of a spheroid in contact with a tip-less **AFM** cantilever. d) (A) **Microtweezer** set-up and (B) cantilever tips compressing a spheroid. e) Time series of the **micropipette aspiration** of a spheroid for almost 3 hours, and retraction of the tongue as the aspiration pressure is set back to zero. (a) is reprinted and adapted from [76], licensed under CC BY 4.0; (b) is reprinted and adapted from [176], licensed under CC BY 3.0; (c) is reprinted and adapted from [90], Copyright 2021, with permission from Elsevier; (d) is reprinted and adapted from [92], licensed under CC BY 4.0; (e) is reprinted and adapted from [178], Copyright 2017, with permission from Elsevier.

defining the time-dependent mechanics of cells is necessary not only to see how they deform but also to understand how they transduce external mechanical forces into biochemical-signaling cascades that govern their behavior [80]. Secondly, changes in a cell's deformability defined by cytoskeletal dynamics have long been considered as a biophysical marker with diagnostic and therapeutic potential for malignancy and metastatic ability in cancer cells [81,82].

A common technique to measure the mechanical properties of single cells and tissues is **atomic force microscopy (AFM)**. The high force sensitivity, spatial resolution and compatibility with living samples make AFM an ideal technique for probing local mechanical properties of tissues, with examples ranging from the rat hippocampus to human breast biopsies [14,15,83,84]. Using a cantilever, the tissue in question is indented at several points in an array in order to map out its stiffness. Knowing the spring constant k of the cantilever, the deflection of the cantilever as a function of indentation depth gives an apparent elastic modulus of the tissue. If the indentations are performed at a single low speed of indentation, solely an apparent pseudo-elastic modulus is determined and the viscoelastic behavior of the tissue is neglected [85]. With a sharp AFM tip, the deformation is highly localized and stress dissipation is determined from viscous drag of the cytoskeletal filaments [86], rather than poroelastic effects [87]. To determine the viscoelastic response of cells or tissues, the AFM can be operated in a dynamic mode using sinusoidal oscillations in force/indentation at a functionally relevant frequency (0.5–4 Hz) [88,89]. The main advantage of AFM is its nanometer-scale spatial resolution, which allows AFM to evaluate the mechanical heterogeneity between morphologically distinct regions within small biological samples. However, AFM indentations are limited to small depths (< 10 μm) making it a surface-based technique [83]. For this reason, it is only suitable to create stiffness profiles of the outer proliferation layer of a spheroid (Figure 4(c)) [90,91]. The technique is therefore mostly used on single cells and flat tissues and rarely for spheroids.

Microtweezers are a novel technique that is more suitable to measure the stiffness of 3D spheroids [92]. Mimicking a pair of chopsticks, the spheroid is held between two force-sensing microtweezers and is compressed by displacing one of the tweezers with a piezo-bimorph actuator (Figure 4(d)). The Young's modulus of the spheroid is determined by optically tracking the bending of the tweezers upon spheroid compression with a pattern matching algorithm. The dual cantilevers are easily replaceable and are able to work with forces ranging from less than one hundred nN to one mN. However, the technique requires fabrication of

custom-made tweezers as well as careful calibration of their spring constants with a precision mechanical stage. As microtweezers are a novel technique, it has not yet been widely used.

A common technique to measure cell or nucleus mechanics is **micropipette aspiration (MPA)** [93–95]. Here, a step-wise stress is applied to a single cell by aspirating it with a micron-sized glass pipette which has a radius that is approximately 3–4 times smaller than the diameter of the cell [93]. In case of a multicellular tissue, cell aspiration can be performed on different cells on the surface of the tissue to map variations in cell mechanics, as demonstrated recently for mammalian embryos [96]. When increasing the pipette radius, the technique can be used to measure the collective viscoelastic properties and surface tension of spheroids [97,98]. Here, a constant stress is applied through an underpressure in the pipette after which a tissue tongue flows into the pipette (Figure 4(e)). Assuming that spheroids behave as viscoelastic drops when exposed to a suction force, the response of the spheroid to the aspiration is characterised by tracking the length of the advancing tongue as a function of the applied underpressure. A drawback to this technique is that it is time-consuming to fabricate the micropipettes and align these with the spheroids.

Interestingly, Guevorkian *et al.* [97] showed how the surface tension of aspirated spheroids increased with the applied force. Retraction of the aspirated cell tongue from the pipette was measured at zero pressure, and shown to be dependent on the applied pressure during the aspiration. In other words, spheroids achieved a *reinforced* tissue cohesion after applying a stress, indicating that the cells actively sense and respond to an applied load. Similar cell reinforcements in response to mechanical perturbations have been found in experiments on single culture cells [99,100]. By contrast, tissue surface tensiometry showed that spheroid surface tensions were independent of the applied force [78]. This discrepancy might be explained by the fact that the aspiration pressure during MPA is only applied to a part of the spheroid, while tissue surface tensiometry exerts a force on the whole spheroid. Future research will have to identify the possible emergence of mechanosensing when applying a local force to a part of the spheroid.

2.3 Probing spheroids from within

2.3.1 Cellular scale

Mechanical features of the local microenvironment are well-established to drive cellular processes [2,3]. Surrounding tissue stiffness affects cell proliferation, migration, differentiation during development [101], tissue homeostasis [102] and disease progression [103,104]. However, techniques to measure mechanical properties of cells and the extracellular matrix inside tissue are limited. Macroscale tools like TST and MPA are not able to

capture local mechanical variations around cells in the interior of a spheroid, as they only measure mechanics of a collective whole from the outside.

An interesting technique to measure the elastic modulus of spheroids from within is **cavitation rheology**, which compares the work of bubble formation to the deformation of the spheroid [50,105]. A spheroid is transferred into a glass capillary, after which a micron-sized glass needle is inserted into the spheroid using a micro-manipulator (Figure 5(a)). By injecting a cavitation medium (air or water), slow pressurization induces an elastic instability in the form of a cavity. The pressure-growth relationship for this induced spherical bubble relates to the elastic modulus of the spheroid [105,106]. Additionally, comparing the energy associated with bubble formation to the binding energies of the cell surface proteins gives an estimation of the cortical tension of the cells that form the spheroid [50]. During measurements, spheroids are kept in culture medium, which introduces a technical challenge since they can float away from the needle during insertion. Moreover, determined elastic modulus values are only valid in the 'thickshell' regime, where the induced cavities are small enough so as to not affect the outer diameter of the spheroid.

Similar to tissues, ECMs exhibit viscoelasticity, mechanical plasticity and nonlinear elasticity, which affect fundamental cellular processes including proliferation, differentiation and migration [107]. When cancerous spheroids are embedded in an ECM scaffold, they remodel the matrix either through contractility or growth, depending on various parameters such as cell type, cellular packing density and ECM stiffness [108–110]. Some cell types form spheroids that, when embedded in collagen gels, induce a contractile pressure at the spheroid-ECM interface, thereby deforming the collagen network inward resulting in tensile forces in the matrix that realign fiber bundles enabling cell invasion [108]. Others form spheroids that grow through cell proliferation, inducing a compressive stress at the spheroid-ECM interface [109,110]. This stress inhibits cell proliferation but is reversible once the stress is released [111]. In order to measure these highly local tissue mechanics, recent studies have developed the use of **hydrogel mechanosensors** [112,113]. In contrast to cavitation rheology which actively probes spheroids, these sensors are used for passive probing. Mechanically well-defined elastic polyacrylamide (PAA) microbeads serve as internal cell-like sensors by being incorporated in spheroids grown under mechanical stress (Figure 5(b), left panel) [113]. They are functionalized to promote cellular adhesion, show fluorescence when imaged, and exhibit uniform and well-calibrated elastic properties. The use of PAA gels provides several advantages. Firstly, the elastic modulus can be easily tuned by changing the relative concentration of acrylamide to bisacrylamide [114]. Furthermore, the material is itself inert so cell adhesion only depends on the

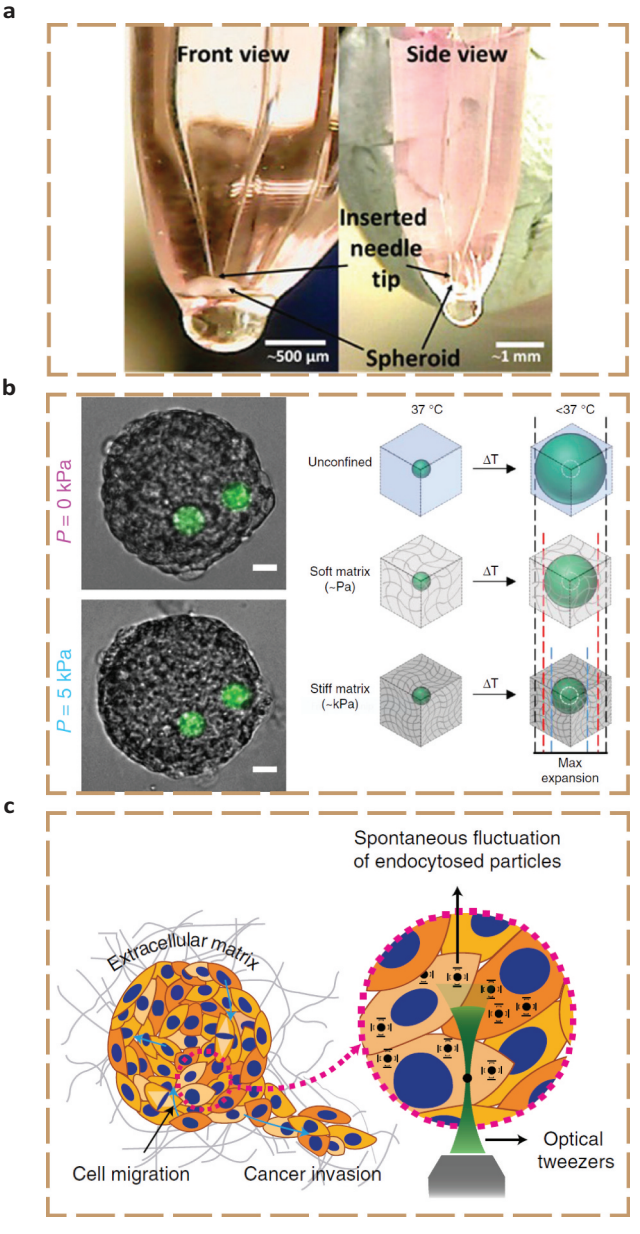

Figure 5. Probing spheroids from within. a) **Cavitation rheology**, where a 30 µm needle is inserted into a spheroid to induce a cavity. b) **Hydrogel mechanosensors**, which can either be osmotically compressed (left, scale bar: 20 µm) or are thermoresponsive (right). Their final change in volume is determined by the elasticity of the surrounding tissue. c) Schematic of a spheroid embedded in ECM, where the cytoplasmic mechanics of the periphery cells are determined using **optical tweezers** pulling on endocytosed particles. (a) is reprinted and adapted from [50], licensed under CC BY 4.0; (b) is reprinted and adapted, the left half from [113] and the right half from [112], both licensed under CC BY 4.0; (c) is reprinted and adapted by permission from Springer Nature: Springer *Nature Physics* [124], Copyright 2020.

type of ligand coupled to the bead's surface. The local pressure inside the spheroid is measured by monitoring the strain (change in volume) of the hydrogel beads. The bulk modulus of the beads can be calibrated beforehand by osmotic compression, for instance with high molecular weight dextran that neither penetrates the beads nor the spheroid [90,115]. At small enough compressions (i.e. small dextran concentrations), the stress/strain relation is linear and the bulk modulus of the beads can be deduced from the slope of the curve. Outside this linear regime, an empirical polynomial Mooney-Rivlin model is used [113]. After determining the bulk modulus of the beads, the pressure profile of the spheroid can be quantified based on before-and-after measurements of the incorporated bead size when osmotically compressing a spheroid. The ideally random distribution of PAA beads across the spheroid enables the determination of the pressure profile along the spheroid radius. Measurements demonstrated that the pressure rises towards the core of the spheroid, explained by the anisotropic arrangement of cells.While these sensors have so far solely been used to identify local pressures in spheroids under isotropic compression, they should also give access to shear stress measurements once the deformation of the beads under shear is identified. Furthermore, anisotropic stresses have been measured in tissues (though not in spheroids) using oil microdroplets functionalized with ligands for cell surface receptors [116]. Similar to the PAA gels, the deformation from their spherical shape at equilibrium translates to force measurements. However, their lack of compressibility makes them unsuitable to identify the isotropic component of the stress.

Recently, a similar type of mechanosensor has been introduced which is temperature-actuated [112]. Unlike PAA, poly N-isopropylacrylamide (PNiPAAM) hydrogels are thermoresponsive gels that remain compact at tissue culture temperatures but swell when cooled by a few degrees (Figure 5 (b), right panel). They can be conceptualized as springs that are pre-loaded by thermodynamic expulsion of water before incorporation in the tissue. Decreasing the temperature releases this pre-strain and returns the beads to a new equilibrium volume defined by the rigidity of the surrounding tissue. The change in volume relates to the elasticity of the tissue after creep. These probes could even be injected within *in vivo* mouse tumors where they did not result in signs of additional fibrosis or inflammation over a period of 3 weeks, suggesting their excellent biocompatibility [112]. The PNiPAAM beads are calibrated by encapsulating them in stiffness-tunable polyacrylamide gels with linear elastic properties and measuring their change in radii after releasing the pre-strain.

However, both hydrogel mechanosensors present some limitations. First, the obtained spatial distribution of mechanical stress in tissues lacks a time-dependent component. Secondly, the sensors may be sensitive to local environmental factors such as pH, which can be nonuniform in spheroids

[117]. Thirdly, both sensors might affect cell behavior as they are foreign particles and induce a foreign body response [118]. Yet, functionalizing the hydrogel surface with appropriate matrix molecules might provide a way to minimize this. Fourthly, the change in temperature needed for PNiPAAM to obtain the measurement may influence the tissue stiffness, though previous studies have shown that cellular rigidity is not significantly affected between 21 °°C and 37°°C [119]. Despite these limitations, the probes provide a unique technique to obtain direct *in situ* mechanical measurements inside spheroids and tissues.

2.3.2 Subcellular scale

Optical tweezers are able to study mechanics within spheroids incorporated in an ECM. While both cavitation rheology and hydrogel mechanosensors probe spheroids at the cellular level, optical tweezers operate at a subcellular level. Optical tweezers have been widely used, in combination with nano- and microfluidics, both in the soft matter field [120] and in biological sciences [121]. The technique uses strongly focused laser light to trap a refractive particle in the focal point [122], providing excellent resolution in positioning ($\pm$ 1 nm) micron-sized particles and in contactless measuring of forces ($\pm$ 50 fN) [123]. Recently, optical tweezers have been used to perform active microrheology on migrating cells in the periphery of a spheroid embedded in a collagen matrix (Figure 5(c)) [124]. The mechanical properties of the cytoplasm inside the peripheral cells were measured by embedding small latex particles in the gel that got endocytosed. The force-displacement curve measured upon dragging the particles with the optical tweezer reveals the cytoplasmic stiffness. Importantly, the method is insensitive to the mechanics of the actin cortex that underlies the membrane, which is a principal determinant of cell surface tension. Additionally, a cell's interior is heterogeneous so care needs to be taken when determining which cellular components regulate the response. Nevertheless, this technique arguably brings us the closest to understanding sub-cellular mechanics inside cell spheroids.

3 From cell sorting to invasion

3.1 Coaction of intercellular adhesion and cortical tension

Cell-cell adhesion is mediated by transmembrane proteins called cadherins that interact through extracellular domains [125]. Cadherin bonds are stabilized by the cortical actin network, with the interaction between actin and cadherins being dynamic and mechanoresponsive [126–128]. Cadherins also act as signaling molecules that begin local reorganization of actomyosin when cells come into contact [129]. While the previously

discussed DAH has successfully accounted for many observations of tissue sorting, it focuses solely on cell adhesion contributions from cadherins to tissue surface tension, and neglects the role of the cortical actin network [70]. Studies following up on the DAH have however shown that the tissue surface tension actually depends on a balance of adhesion, cortical tension and cortical elasticity [130–132]. These findings helped shape the differential interfacial tension hypothesis (DITH), which relates tissue surface tension to the tension along individual cell-cell interfaces and to the role of actin-myosin activity (Figure 6(a)). The DITH acknowledges that individual cells are not point objects but finite-sized deformable objects that can adapt their geometry. Since the mechanical energy changes with cell shape, the cortical tension evoked by the thin cortical layer of actin beneath the cell membrane has to be involved in the energy balance [133]. To resolve possible discrepancies between the DAH, which states that cell types sort due to cadherin ratios (Figure 6(b)), and the DITH, Manning *et al.* developed a model that explicitly showed how the overall surface tension of a multicellular aggregate is determined by the ratio of adhesion tension to cortical tension, indicating a crossover from adhesion-dominated to cortical tension-dominated behavior [20].

To experimentally demonstrate the coaction of cell adhesion and cortical tension in determining tissue surface tension, Manning *et al.* treated spheroids made of mouse embryonic fibroblasts transfected with P-cadherin with actin-depolymerizing drugs (cytochalasin D and latrunculin A), making the cells not only lose cortical tension but also cell-cell adhesion as the actin anchor of cadherin bonds was weakened [20]. This drug treatment resulted in rounded surface cells and a lower surface tension of the spheroid in contrast to untreated control spheroids that had flat cells at the surface that were stretched across multiple bulk cells in order to maximize cell-cell contact (Figure 6(c)). This finding demonstrated how changes in surface cell shape influence tissue surface tension. When the surface cells are compact, they make fewer adhesive contacts than the bulk cells, and this differential adhesion is the primary contribution to the surface tension just as in liquids. In this scenario, the surface tension varies linearly with the *effective* adhesion as predicted by the DAH. However, the comparison to fluids becomes invalid once surface cells elongate so they can make contacts with multiple bulk cells. In this case, there is no longer an adhesive contribution to the surface tension and the DAH breaks down. The ratio between cortical tension and effective adhesion will determine whether surface tension is in a regime where intercellular adhesion is dominant or in one where cortical tension dominates.

While the DAH and DITH are based on the assumption that all cells are roughly identical and can be characterized by properties measured for a single cell, cells at tissue boundaries mechanically differ from those in the interior [134,135]. Boundary cells actively change their mechanical

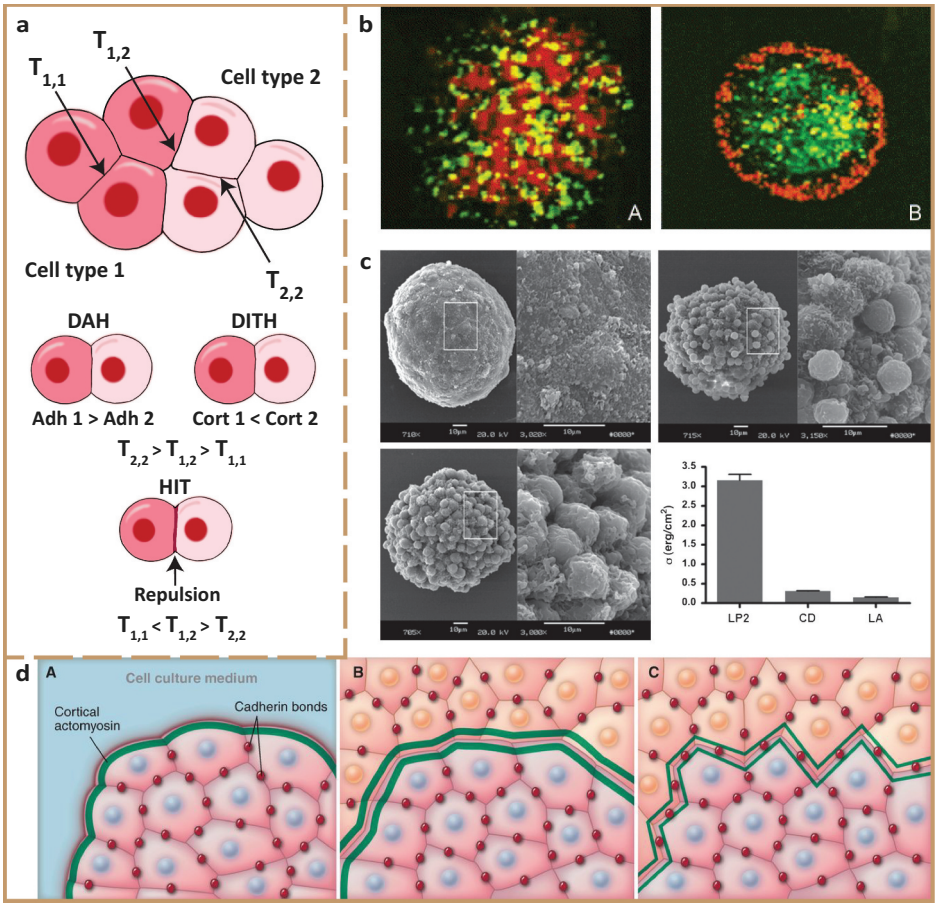

Figure 6. Cell sorting and tensions. a) Schematic of contact tension in tissues, and the three main models for cell sorting, showing differences in homotypic tensions $T_{1,1}$ and $T_{2,2}$ and heterotypic tension $T_{1,2}$. The DAH is regulated by cell adhesion, while the DITH also involves the role of cytoskeletal components, and the HIT focuses on repulsive mechanisms generated by ephrin-Eph signalling. For the DAH and DITH, heterotypic tensions are intermediate, in contrast to the HIT where they exceed the homotypic tensions. Inspired by [140]. b) Confocal images of a spheroid made from two cell lines transfected to have different N-cadherin ratios. First, (A) the spheroid remains mixed after 4 h of incubation (B) but after 24 h sorts in accordance with the DAH, with the cell line expressing the lower level of N-cadherin (red) enveloping the cell line expressing higher amounts of N-cadherin (green). c) SEM images of spheroids made from a P-cadherin-transfected L-cell line termed LP2 by the authors; with up-left a control LP2 aggregate, up-right treated with latrunculin A (LA) and down-left treated with cytochalasin D (CD) to depolymerize actin. Down-right shows surface tensions σ measured for all three types with tissue surface tensiometry. d) Boundary polarization at (A) tissue-culture and (B, C) tissue-tissue interface. Red dots indicate cadherin bonds, green lines indicate higher-than-average actin density where the thickness of the line shows the amount of generated tension. Nuclei are either blue or orange to make a distinction between two cell types. While boundary polarization occurs for tissues in vitro, it (B) may or (C) may not occur at an *in vivo* tissue-tissue interface, possibly explaining differences between *in vivo* and *in vitro* cell sorting. (b) is reprinted from [70], Copyright 2005, with permission from Elsevier; (c) is reprinted from [20], with permission from the authors; (d) is reprinted from [129]. Reprinted with permission from AAAS.

properties; they mechanically polarize [129]. Using traction force microscopy, cells in pairs and triplets plated on collagen-coated polyacrylamide gels were shown to reorganize their adhesive and cytoskeletal properties. The cells displayed a significantly higher density of actin filaments and a higher tension along the external boundary interfaces compared to the internal interfaces of the pairs and triplets [136]. With increasing 2D cohesive colony size (up to 27 cells) on soft substrates, traction stresses localized at the edge of the colony, demonstrating mechanical polarization at tissue boundaries [134]. Boundary polarization also occurs *in vivo*, for example at compartment boundaries in the *Drosophila* embryo [137,138]. However, the possible relation between mechanical polarization and tissue sorting remains unclear. Tissue compartmentalization *in vivo* does not always correlate with *in vitro* cell sorting, as has been shown in *Xenopus* embryos [139]. While *in vitro* cell sorting is dominated by short-time scale interactions between the external domains of cadherins, *Xenopus* embryo results suggest that *in vivo* sorting is regulated by long-time scale spatial reorganization of cadherins and cortical tension upon tissue intercalation [139]. The inconsistency between *in vitro* and *in vivo* cell compartmentalization might occur because contact with culture medium for *in vitro* cell aggregates will necessarily mechanically polarize the system (Figure 6(d)). Next to this, cells *in vivo* are in contact with complex extracellular matrix structures, which may influence boundary polarization and thereby cell sorting.

Although differences in cell adhesion and cortical tension suffice to drive cell sorting *in vitro*, recent experiments show that a local discontinuity in contact tension is an additional requirement to build an embryonic boundary and induce tissue separation *in vivo* [140]. In embryonic tissues, membrane-bound proteins such as ephrins and Eph receptors induce local repulsion at heterotypic contacts between different cell types and thereby efficiently sort cell populations and inhibit mixing [141]. This discovery gave birth to the high heterotypic interfacial tension (HIT) model, where ephrin-Eph-mediated repulsion creates a higher tension at the heterotypic boundary between two tissues compared to the tensions at the homotypic contacts inside each separate tissue (Figure 6(a)). This differs from the DAH and DITH, which assume that the homotypic tension is higher in one of the two cell populations and intermediate at the heterotypic boundary [140]. Computer simulations suggest that the most favourable condition for tissue separation is to have low contact tension (the sum of the two cortical tensions at a cell-cell contact) in both tissues that contrasts with the high interfacial tension between the tissues [140]. The strength of cell-cell adhesions within tissues is therefore important for tissue separation as long as it creates the correct difference in tension with the heterotypic interfacial tension. The simulations were confirmed by experiments using *Xenopus*

embryonic cell types [140]. Tissue separation still occurred when one of the homotypic tensions was equal to or even higher than the heterotypic tension, as long as this difference was compensated by a large difference between the heterotypic and second homotypic tension. The DAH and DITH assume that tissues are liquid-like and sample many configurations until they find the minimum free energy states. Kinematic effects such as active cell motility and cell shape fluctuation are assumed to be sufficiently small such that the system dynamics are governed by a free energy [129]. These assumptions have been challenged by experiments in which small changes to single-cell properties caused tissues to transition from a liquid-like to a solid-like state, termed as jamming [142]. The other way around, epithelial cells that are first in a solid-like jammed state can start to exhibit a collective phase that is dynamic, migratory and fluid-like, termed unjammed [143]. Both *in vivo* and *in vitro*, for example for primary human bronchial epithelial cells, cell shapes become more elongated and more variable as the epithelial layer becomes more unjammed [143,144]. This change in cell shape, parameterized through a shape index, reflects the competition between cell-cell adhesion and cortical tension during the jamming/unjamming transition [142,144,145]. Here, rearrangements amongst neighboring cells are seen to be hindered by local energy barriers, defined by a combination of cell-cell adhesion, cortical tension and cellular propulsion. When the propulsive forces are negligible, theory describes how an increase in cell-cell adhesion or decrease in cortical tension can cause energy barriers to decrease or disappear [142,144,145]. When this happens, cells unjam. In the process of metastasis, cells usually change their adhesion and cortical tension. In order to migrate, tumour cells lose epithelial characteristics and obtain a more mesenchymal phenotype [146,147]. This change in characteristics is called the epithelial-mesenchymal transition (EMT). Once tumour cells have metastasized into the secondary organ environment, the reverse process can occur (for example through re-expression of E-cadherin) and the cells undergo a mesenchymal-epithelial transition (MET) [148]. Even though epithelial cells are endowed with plasticity and increased migratory capacity during both EMT and unjamming, the cellular crowded, solid-like epithelial collective can undergo unjamming in the absence of EMT [149]. Changes in EMT marker protein levels like E-cadherin, vimentin and N-cadherin do not correlate with unjamming migratory dynamics [150]. Even more, in forms such as breast cancer, lung cancer and prostate cancer, metastasis is dominated not by dispersion of individual cells but rather by collective migration of clusters, packs or strands [151,152]. To remain in these clusters, carcinoma cells often stay cohesive and continue to express epithelial markers such as E-cadherin [153,154]. A recent study with spheroids showed how cell sorting changes depending on the metastatic properties of cancer cells,

Box: definitions of mechanical parameters characterizing cell spheroids

Cortical tension

The apparent surface tension of a cell, presumed to be dominated by myosin motor-driven contraction of the actin cortex and the interaction of the actin cortex with the membrane. SI unit: N/m.

Stress

Force exerted on a surface area. The direction at which the force is applied to the area determines whether it is a compressive stress (perpendicular to the surface), shear stress (parallel to the surface) or elongational stress (perpendicular to the surface). SI unit: Pa.

Strain

The amount by which a material is deformed. Strain is determined from the change in size of the material before and after a force is applied. Unitless.

Elasticity

The instantaneous response of a material to force by deforming a certain amount that is proportional to the applied stress. An elastic material maintains its deformation while under stress and recovers to its original shape once the stress is removed. A material's 'spring constant' is normally quantified by the elastic modulus, which is the ratio of stress to strain. Depending on how stress and strain directions are specified, three primary moduli are defined: the *Young's modulus* is the ratio of tensile stress to tensile strain, when the object deforms along the same axis of applied forces; the *shear modulus* is the ratio of shear stress to shear strain, when the object shears and deforms at constant volume; the *bulk modulus* is the ratio of volumetric stress to volumetric strain, when the object deforms in all directions when uniformly loaded in all directions. SI unit: Pa.

Viscosity

Response of a material to force by deforming without limit at a rate which is proportional to the stress. A liquid increases its deformation in proportion to the duration of the applied stress, and does not recover its original size/shape once the stress is removed. SI unit: Pa s.

Viscoelasticity

Most soft materials have both elastic and viscous responses, making them viscoelastic. When subjected to a stress, they deform at a rate which is not simply linearly proportional to the stress and partially recover their shape once the stress is removed. Cellular viscoelastic behavior is often phenomenologically described in terms of a network of elastic springs and viscous dashpots connected either in series or in parallel, depending on the model. The creep and stress relaxation of single cells in reality often displays a power law behavior indicating a continuous distribution of timescales [86,171,172]. Yet for tissue-level mechanics, the debate on whether power laws describe their viscoelastic response accurately enough is ongoing. As an example, power laws are insufficient to describe the viscoelastic behavior of muscle tissue as it demonstrates a broad distribution of timescales around a characteristic time constant determined by acto-myosin activity [173]. Nevertheless, spring-dashpot models with characteristic timescales remain useful in soft tissue mechanics to extract viscoelastic parameters [97].

Tissue fluidity

Cell motility corresponding to a fluidization of the tissue on the bulk level. When cells readily rearrange and are migratory, the tissue is considered to be fluidlike or unjammed. Here, cells often migrate in multicellular packs and swirls reminiscent of fluid flow. In contrast, when cells are locked in their positions and often have compact shapes, the tissue is called solidlike or jammed [143,144,150].

Tissue surface tension

An analogy is made between tissues and liquids, where liquids have a surface tension which equals the free-energy change when the liquid surface is increased by a unit area. Tissues also have an apparent surface tension, which arises from the adhesive interactions between cells and their cortical tensions. SI unit: N/m.

relating to active cell motility, EMT and jamming [135]. The study analyzed the mechanical properties of three breast cancer cell lines (MCF-10A, MDA-MB-231, MDA-MB-436), selected because they cover a shift in E-, N- and P-cadherin levels characteristic of EMT, mixed the cell lines to form heterogeneous spheroids and looked at the sorting behavior. Surprisingly, the final sorted states of the grown spheroids proved to be incorrectly predicted by the DAH as cell lines with a lower surface tension would not always envelop the ones with a higher surface tension. In contrast to embryonic tissues that do sort in agreement with the DAH [65], cell lines that demonstrate EMT-characteristics apparently do not have to follow

these models. Instead of behaving as simple liquids, active cell motility and processes such as cell jamming may play an important part in tissue sorting across the epithelial-mesenchymal transition. Dynamical effects such as directional motility, friction and jamming are therefore of importance when investigating sorting in multicellular tumour spheroids.

3.2 Spheroid mechanics and cell migration

The architecture of heterogeneous spheroids not only defines their surface tension but also critically influences the detachment of cells from the spheroid and cell invasion into the surrounding extracellular matrix. For example, the sorting of heterogeneous spheroids (1:1 ratio metastatic MDA-MB-231 and non-tumorigenic MCF-10A cells) embedded in a collagen matrix modulated the speed, persistence and mean squared displacement of the MDA-MB-231 malignant breast tumour cells (Figure 7(a)) [155]. At approximately 4 days of growth, MCF-10A cells enclosed the MDA-MB-231 cells in the core of the spheroid due to their higher proliferation rate, pointing out how proliferation plays an additional role in cell sorting. The confinement prevented the malignant MDA-MB-231 cells from invading outwards, demonstrating the potential influence of cell sorting on cancer metastasis.

Cells in 3D display multiple modes of migration, among which mesenchymal, amoeboid, lobopodial and collective, depending on the local extracellular microenvironment [156]. They can switch between mesenchymal migration mechanisms depending on lamellipodia, thin membrane protrusions found at the leading edge of migrating cells, and alternative migration mechanisms such as amoeboid migration, characterized by a rounded cell morphology with low adhesive interactions, depending on the degree of confinement they experience [157]. The nucleus serves as an intracellular mechano-gauge during these shape deformations [158]. It senses imposed constraints through an increase in nuclear membrane tension, triggering signaling outputs that increase cell migratory capacity through actomyosin contractility, thus linking mechanics to migration [159].

The tumour microenvironment also plays an important role in cell metastasis for spheroid models [34,107,160–162]. For example, interstitial flows can downregulate the cell-cell adhesion molecule E-cadherin on non-tumorigenic cells and promote spheroid invasion [163]. Furthermore, the choice of surrounding ECM type and density in spheroid invasion assays also influences cell mechanics and migration. *In vivo*, interstitial stromal ECM is a heterogeneous fibrillar network of primarily type I collagen [107]. *In vitro*, the incorporation of epithelial cell aggregates in type I collagen induces mesenchymal gene expression and an invasive phenotype. By contrast, epithelial cells incorporated in Matrigel remain non-invasive [164]. In

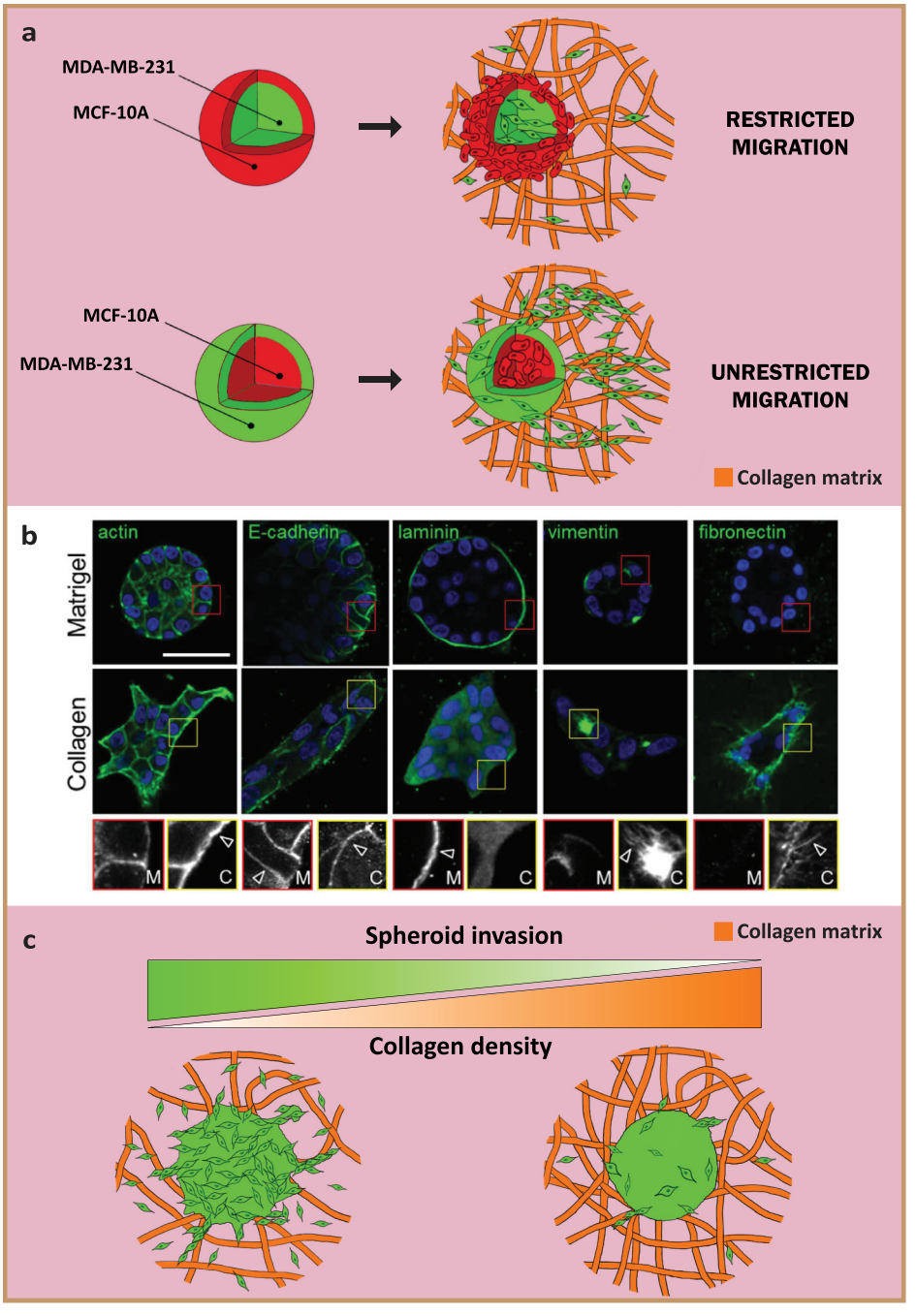

Figure 7. Spheroid cell invasion. a) Architecture of heterogeneous spheroids (MDA-MB-231: green and MCF-10A: red) influences cell invasion in collagen matrix. Malignant MDA-MB-231 cells are able to invade collagen when on the outside of the spheroid, but are constricted and (mostly) prevented from migrating when the non-tumorigenic MCF-10A cells enclose the malignant core. Inspired by [155]. b) Spheroid microenvironment is involved in metastatic gene expression. Confocal images of actin, E-cadherin, laminin, vimentin and fibronectin in cell aggregates embedded in gels show an increase in mesenchymal markers and invasion when in collagen compared to Matrigel. Insets and arrows point out changes in Matrigel (red) and

collagen (yellow). Scale bar: 50 μm. c) Collagen density influences spheroid invasion and distinct modes of migration. Single-cell migration dominates at low collagen densities (~1 mg/ml), while collective migration orchestrates invasion in higher collagen densities (~ 4 mg/ml). Inspired by [165]. (b) is reprinted and adapted from [164], licensed under CC BY 4.0.

mixtures of collagen and Matrigel, non-tumorigenic MCF-10A breast cancer aggregates become increasingly invasive as the relative collagen content is increased by downregulating their E-cadherin expression while increasing mesenchymal markers like vimentin, fibronectin and Snail (Figure 7(b)). Depending upon cell type and matrix density, cells at the periphery of spheroids embedded in type I collagen switch between distinct modes of invasion in a manner that is reminiscent of a non-equilibrium phase separation [165]. Low collagen densities result in a locally unjammed invasive periphery resembling a fluid-like phase, while high collagen densities ensure non-invasive solid-like behavior (Figure 7(c)). Here, collagen densities define cell volume, shape and motility, making heterogeneities within the spheroid not only regional or subclonal but also mechanical. Within a multicellular tumour spheroid, the core is approximately jammed and solid-like (rounded cell shapes and limited cell motion) while the periphery of the tumour is more fluid-like (elongated cell shapes and larger cell motion) [124,166]. Han *et al.* used the previously mentioned optical tweezer technique to perform active microrheology on embedded spheroids and demonstrated how the variability in stiffness of different cells within the population increased as the spheroid matured over time. They seeded spheroids in a 3D hydrogel network composed of alginate and Matrigel with a shear modulus of approximately 300 Pa, thus mimicking the mechanical microenvironment of a breast carcinoma *in vivo* [103,124]. In terms of cell mechanics, cells at the spheroid periphery and invasive branches tended to be softer, larger, longer and more dynamic compared to the cells in the core. Subsequently, they demonstrated how these mechanical changes arise in part from supracellular fluid flow through gap junctions that allow exchange of ions and fluids between cells and amplify cell volume variations in tumours [167]. Blocking these junctions delayed the transition of cells at the periphery into an invasive phenotype. As swelling and softening of peripheral cells are important factors in invasive dynamics, the authors sought to artificially manipulate cell stiffness and volume. Using the chemotherapy medication daunorubicin or overexpression of the actin cross-linking protein -actinin, the cytoplasmic stiffness of the cells was increased, which diminished invasion of peripheral cells. Invasiveness was quantified as the percentage of spheroids forming invasive branches after 11 days. It will be interesting in the future to explore these effects for different cancer cell types and as a function of ECM composition, in order to better understand the biophysical cues that govern metastasis.

4 Conclusions and outlook

Current strategies for the mechanical characterization of 3D multicellular spheroids allow us to understand how mechanical forces regulate tissue formation, cell sorting and cell migration. While several new tools introduced here enable identification of spheroid mechanics both from without and within, a technique that visualizes active mechanosensitive reinforcement of cells and cell-cell contacts is still missing. Furthermore, correlative imaging and multiscale mechanical measurements are needed to deconvolve the contribution of the actomyosin cortex and cell-cell adhesion to overall tissue mechanics. A new noninvasive method to help with this could be CellFIT-3D, a force inference technique that estimates tension maps for 3D cellular systems from image stacks [168]. In addition, artificial intelligence algorithms have been implemented on traction force microscopy to evaluate and predict cellular forces after sufficient training from captured images [169]. This new machine learning-based approach has great potential for being implemented in biophysical tools and invasion assays for more high-throughput and accurate biophysical characterization of spheroids and cell migration. Besides actin and cadherin, the role of other cytoskeletal elements in cell invasion remains largely unexplored. It would be particularly interesting to study the role of intermediate filaments, a family of cytoskeletal filaments that are expressed in a tissue-specific manner. Upon the epithelial-mesenchymal transition, expression of intermediate filaments switches from keratin to vimentin [170]. The mechanical consequences of this switch at the multicellular level are to be identified. Additionally, what physical mechanisms determine whether cells leave individually or as collective strands remains an open question to be further investigated. In summary, identifying the precise relation between spheroid mechanics, cell invasion and involved biological processes will provide new opportunities to understand tissue and cancer biology, and can reveal targets for therapeutic strategies for cancer treatment.

Acknowledgments

R.C.B. and P.E.B. gratefully acknowledge the funding from the European Research Council (ERC) under the European Union's Horizon 2020 research and innovation programme (grant agreement no. 819424). G.H.K. gratefully acknowledges funding from the VICI project How cytoskeletal teamwork makes cells strong (project number VI.C.182.004) which is financed by the Dutch Research Council (NWO).

Funding

This work was supported by the European Research Council (ERC) [819424]; Nederlandse Organisatie voor Wetenschappelijk Onderzoek [VI.C.182.004].

ORCID

Ruben C. Boot http://orcid.org/0000-0003-4003-8276
Pouyan E. Boukany http://orcid.org/0000-0002-2262-5795

References

[1] Vogel V, Sheetz M. Local force and geometry sensing regulate cell functions. Nat Rev Mol Cell Biol. 2006;7:265–275.
[2] Discher DE, Mooney DJ, Zandstra PW. Growth factors, matrices, and forces combine and control stem cells. Science. 2009;324:1673–1677.
[3] Van Helvert S, Storm C, Friedl P. Mechanoreciprocity in cell migration. Nat Cell Biol. 2018;20:8–20.
[4] Bodor DL, Pönisch W, Endres RG, et al. Of cell shapes and motion: the physical basis of animal cell migration. Dev Cell. 2020;52:550–562.
[5] Wozniak MA, Chen CS. Mechanotransduction in development: a growing role for contractility. Nat Rev Mol Cell Biol. 2009;10:34–43.
[6] Tajik A, Zhang Y, Wei F, et al. Transcription upregulation via force-induced direct stretching of chromatin. Nat Mater. 2016;15:1287–1296.
[7] Mammoto T, Ingber DE. Mechanical control of tissue and organ development. Development. 2010;137:1407–1420.
[8] Brugués A, Anon E, Conte V, et al. Forces driving epithelial wound healing. Nat Phys. 2014;10:683–690.
[9] Hahn C, Schwartz MA. Mechanotransduction in vascular physiology and atherogenesis. Nat Rev Mol Cell Biol. 2009;10:53–62.
[10] Nia HT, Liu H, Seano G, et al., L Steele Laboratories, Massachusetts General, Translational Medicine, Biomedical Sciences, Biological Engineering, Hospital S Joao, Oncology Service, Connective Tissue Oncology, and Massachusetts General Hospital. Solid stress and elastic energy as measures of tumour mechanopathology. Nat Biomed Eng. 2016;1:1–25.
[11] Nia HT, Munn LL, Jain RK. Physical traits of cancer. Science. 2020;370:eaaz0868.
[12] Mierke CT. The matrix environmental and cell mechanical properties regulate cell migration and contribute to the invasive phenotype of cancer cells. Rep Prog Phys. 2019;82:064602.
[13] Muiznieks LD, Keeley FW. Molecular assembly and mechanical properties of the extracellular matrix: a fibrous protein perspective. Biochim Biophys Acta, Mol Basis Dis. 2013;1832:866–875.
[14] Schiele NR, Von Flotow F, Tochka ZL, et al. Actin cytoskeleton contributes to the elastic modulus of embryonic tendon during early development. J Orthop Res. 2015;33:874–881.
[15] Marturano JE, Arena JD, Schiller ZA, et al. Characterization of mechanical and biochemical properties of developing embryonic tendon. Proc Natl Acad Sci U S A. 2013;110:6370–6375.
[16] Trepat X, Sahai E. Mesoscale physical principles of collective cell organization. Nat Phys. 2018;14:671–682.
[17] Hall JB, Mcneil SE, Kreutz W, et al. Soft matter models of developing. Science. 2012;82:910–917.
[18] Kim J, Koo BK, Knoblich JA. Human organoids: model systems for human biology and medicine. Nat Rev Mol Cell Biol. 2020;21:571–584.

[19] Barone V, Heisenberg CP. Cell adhesion in embryo morphogenesis. Curr Opin Cell Biol. 2012;24:148–153.
[20] Lisa Manning M, Foty RA, Steinberg MS, et al. Coaction of intercellular adhesion and cortical tension specifies tissue surface tension. Proc Natl Acad Sci U S A. 2010;107:12517–12522.
[21] Rossi G, Manfrin A, Lutolf MP. Progress and potential in organoid research. Nat Rev Genet. 2018;19:671–687.
[22] Riccobelli D, Bevilacqua G. Surface tension controls the onset of gyrification in brain organoids. J Mech Phys Solids. 2020;134:103745.
[23] Balbi V, Destrade M, Goriely A. Mechanics of human brain organoids. Phys Rev E. 2020;101:1–8.
[24] Rozman J, Krajnc M, Ziherl P. Collective cell mechanics of epithelial shells with organoid-like morphologies. Nat Commun. 2020;11:1–9.
[25] Jakab K, Damon B, Doaga O, et al. Relating Cell and Tissue Mechanics: implications and Applications. Dev Dyn. 2008;237:2438–2449.
[26] Sadati M, Qazvini NT, Krishnan R, et al. Collective migration and cell jamming. Differentiation. 2013;86:121–125.
[27] Camley BA, Rappel WJ. Physical models of collective cell motility: from cell to tissue. J Phys D Appl Phys. 2017;50:113002.
[28] Matoz-Fernandez DA, Agoritsas E, Barrat JL, et al. Nonlinear rheology in a model biological tissue. Phys Rev Lett. 2017;118:1–5.
[29] Ranft J, Basan M, Elgeti J, et al. Fluidization of tissues by cell division and apoptosis. Proc Natl Acad Sci U S A. 2010;107:20863–20868.
[30] Merkel M, Lisa Manning M. Using cell deformation and motion to predict forces and collective behavior in morphogenesis. Semin Cell Dev Biol. 2017;67:161–169.
[31] Oswald L, Grosser S, Smith DM, et al. Jamming transitions in cancer. J Phys D Appl Phys. 2017;50:483001.
[32] Mandadapu KK, Govindjee S, Mofrad MRK. On the cytoskeleton and soft glassy rheology. J Biomech. 2008;41:1467–1478.
[33] Kollmannsberger P, Fabry B. Linear and nonlinear rheology of living cells. Annu Rev Mater Res. 2011;41:75–97.
[34] Olga Ilina PG, Gritsenko SS, Lippoldt J, et al. Cell–cell adhesion and 3D matrix confinement determine jamming transitions in breast cancer invasion. Nat Cell Biol. 2020;22:1103–1115.
[35] Angelini TE, Hannezo E, Trepatc X, et al. Glass-like dynamics of collective cell migration. Proc Natl Acad Sci U S A. 2011;108:4714–4719.
[36] Nath S, Devi GR. Three-dimensional culture systems in cancer research: focus on tumor spheroid model. Pharmacol Ther. 2016;163:94–108.
[37] Heisenberg CP, Yohanns B. Forces in tissue morphogenesis and patterning. Cell. 2013;153:948–962.
[38] Gómez-González M, Latorre E, Arroyo M, et al. Measuring mechanical stress in living tissues. Nat Rev Phys. 2020;2:300–317.
[39] Baker BM, Chen CS. Deconstructing the third dimension-how 3D culture microenvironments alter cellular cues. J Cell Sci. 2012;125:3015–3024.
[40] Duval K, Grover H, Han LH, et al. Modeling physiological events in 2D vs. 3D cell culture. Physiology. 2017;32:266–277.
[41] Jensen C, Teng Y. Is it time to start transitioning from 2D to 3D cell culture? Front Mol Biosci. 2020;7:1–15.
[42] Costa EC, Moreira AF, de Melo-Diogo D, et al. 3D tumor spheroids: an overview on the tools and techniques used for their analysis. Biotechnol Adv. 2016;34:1427–1441.

[43] Kelm JM, Timmins NE, Brown CJ, et al. Method for generation of homogeneous multicellular tumor spheroids applicable to a wide variety of cell types. Biotechnol Bioeng. 2003;83:173–180.
[44] Costa EC, Gaspar VM, Coutinho P, et al. Optimization of liquid overlay technique to formulate heterogenic 3D co-cultures models. Biotechnol Bioeng. 2014;111:1672–1685.
[45] Grimes DR, Kelly C, Bloch K, et al. A method for estimating the oxygen consumption rate in multicellular tumour spheroids. J Royal Soc Interface. 2014;11:20131124.
[46] Groebe K, Mueller-Klieser W. On the relation between size of necrosis and diameter of tumor spheroids. Int J Radiat Oncol Biol Phys. 1996;34:395–401.
[47] Jamieson LE, Harrison DJ, Campbell CJ. Chemical analysis of multicellular tumour spheroids. Analyst. 2015;140:3910–3920.
[48] Jain RK, Au P, Tam J, et al. Engineering vascularized tissue. Nat Biotechnol. 2005;23:821–823.
[49] Foty R. A simple hanging drop cell culture protocol for generation of 3D spheroids. J Visualized Exp. 2011;20:4–7.
[50] Blumlein A, Williams N, McManus JJ. The mechanical properties of individual cell spheroids. Sci Rep. 2017;7:1–10.
[51] Shi W, Kwon J, Huang Y, et al. Facile tumor spheroids formation in large quantity with controllable size and high uniformity. Sci Rep. 2018;8:1–9.
[52] Sabhachandani P, Motwani V, Cohen N, et al. Generation and functional assessment of 3D multicellular spheroids in droplet based microfluidics platform. Lab Chip. 2016;16:497–505.
[53] Lee SW, Hong S, Jung B, et al. In vitro lung cancer multicellular tumor spheroid formation using a microfluidic device. Biotechnol Bioeng. 2019;116:3041–3052.
[54] Yeon SE, No DY, Lee SH, et al. Application of concave microwells to pancreatic tumor spheroids enabling anticancer drug evaluation in a clinically relevant drug resistance model. PLoS ONE. 2013;8:1–12.
[55] Kang SM, Kim D, Lee JH, et al. Engineered microsystems for spheroid and organoid studies. Adv Healthc Mater. 2021;10:1–18.
[56] Okuyama H, Kondo J, Sato Y, et al. Dynamic change of polarity in primary cultured spheroids of human colorectal adenocarcinoma and its role in metastasis. Am J Pathol. 2016;186:899–911.
[57] Weaver VM, Petersen OW, Wang F, et al. Reversion of the malignant phenotype of human breast cells in three- dimensional culture and in vivo by integrin blocking antibodies. J Cell Biol. 1997;137:231–245.
[58] Abe-Fukasawa N, Watanabe R, Gen Y, et al. A liquid culture cancer spheroid model reveals low PI3K/Akt pathway activity and low adhesiveness to the extracellular matrix. FEBS J. 2021;Apr 9. doi: 10.1111/febs.15867. Epub ahead of print. PMID: 33837641.
[59] Gomes MD, Iden S. Orchestration of tissue-scale mechanics and fate decisions by polarity signalling. EMBO J. 2021;e106787:1–19.
[60] Riga A, Castiglioni VG, Boxem M. New insights into apical-basal polarization in epithelia. Curr Opin Cell Biol. 2020;62:1–8.
[61] Rodriguez-Boulan E, Macara IG. Organization and execution of the epithelial polarity programme. Nat Rev Mol Cell Biol. 2014;15:225–242.
[62] Zajac O, Raingeaud J, Libanje F, et al. Tumour spheres with inverted polarity drive the formation of peritoneal metastases in patients with hypermethylated colorectal carcinomas. Nat Cell Biol. 2018;20:296–306.

[63] Foty RA, Pfleger CM, Forgacs G, et al. Liquid properties of embryonic tissues: measurement of interfacial tensions. Phys Rev Lett. 1994;72:2298–2301.
[64] Foty RA, Pfleger CM, Forgacs G, et al. Surface tensions of embryonic tissues predict their mutual envelopment behavior. Development. 1996;122:1611–1620.
[65] Schötz EM, Burdine RD, Jülicher F, et al. Quantitative differences in tissue surface tension influence zebrafish germ layer positioning. HFSP J. 2008;2:42–56.
[66] Ayan B, Heo DN, Zhang Z, et al. Aspiration-assisted bioprinting for precise positioning of biologics. Sci Adv. 2020;6:1–17.
[67] Steinberg MS. On the mechanism of tissue reconstruction by dissociated cells. I. Population kinetics, differential adhesiveness. and the absence of directed migration. Proc Natl Acad Sci U S A. 1962;48:1577–1582.
[68] Steinberg MS. Mechanism of tissue reconstruction by dissociated cells, II: time-course of events. Science. 1962;137:762–763.
[69] Steinberg MS. On the mechanism of tissue reconstruction by dissociated cells, III. Free energy relations and the reorganization of fused, heteronomic tissue fragments. Proc Nat Acad Sci. 1962;48:1769–1776.
[70] Foty RA, Steinberg MS. The differential adhesion hypothesis: a direct evaluation. Dev Biol. 2005;278:255–263.
[71] Harris AK. Is cell sorting caused by differences in the work of intercellular adhesion? A critique of the steinberg hypothesis. J Theor Biol. 1976;61:267–285.
[72] Foty RA, Steinberg MS. Cadherin-mediated cell-cell adhesion and tissue segregation in relation to malignancy. Int J Dev Biol. 2004;48:397–409.
[73] Duguay D, Foty RA, Steinberg MS. Cadherin-mediated cell adhesion and tissue segregation: qualitative and quantitative determinants. Dev Biol. 2003;253:309–323.
[74] Kashef J, Franz CM. Quantitative methods for analyzing cell-cell adhesion in development. Dev Biol. 2015;401:165–174.
[75] Kosheleva NV, Efremov YM, Shavkuta BS, et al. Cell spheroid fusion: beyond liquid drops model. Sci Rep. 2020;10:1–15.
[76] Grosser S, Lippoldt J, Oswald L, et al. Cell and nucleus shape as an indicator of tissue fluidity in carcinoma. Phys Rev X. 2021;11:011033.
[77] Dechristé G, Fehrenbach J, Griseti E, et al. Viscoelastic modeling of the fusion of multicellular tumor spheroids in growth phase. J Theor Biol. 2018;454:102–109.
[78] Norotte C, Marga F, Neagu A, et al. Experimental evaluation of apparent tissue surface tension based on the exact solution of the Laplace equation. EPL. 2008;81:46003.
[79] Mgharbel A, Delanoë-Ayari H, Rieu JP. Measuring accurately liquid and tissue surface tension with a compression plate tensiometer. HFSP J. 2009;3:213–221.
[80] Ingber DE. Cellular mechanotransduction: putting all the pieces together again. FASEB J. 2006;20:811–827.
[81] Coughlin MF, Fredberg JJ. Changes in cytoskeletal dynamics and nonlinear rheology with metastatic ability in cancer cell lines. Phys Biol. 2013;10:065001.
[82] Guck J, Schinkinger S, Lincoln B, et al. Optical deformability as an inherent cell marker for testing malignant transformation and metastatic competence. Biophys J. 2005;88:3689–3698.
[83] Elkin BS, Azeloglu EU, Costa KD, et al. Mechanical heterogeneity of the rat hippocampus measured by atomic force microscope indentation. J Neurotrauma. 2007;24:812–822.
[84] Plodinec M, Loparic M, Monnier CA, et al. The nanomechanical signature of breast cancer. Nat Nanotechnol. 2012;7:757–765.

[85] Fung YC. Biomechanics: mechanical properties of living tissues. 2nd ed. New York: Springer-Verlag; 1993.
[86] Fabry B, Maksym GN, Butler JP, et al. Time scale and other invariants of integrative mechanical behavior in living cells. Phys Rev E Stat Phys Plasmas Fluids Relat Interdiscip Top. 2003;68:1–18.
[87] Moeendarbary E, Valon L, Fritzsche M, et al. The cytoplasm of living cells behaves as a poroelastic material. Nat Mater. 2013;12:253–261.
[88] Mahaffy RE, Park S, Gerde E, et al. Quantitative analysis of the viscoelastic properties of thin regions of fibroblasts using atomic force microscopy. Biophys J. 2004;86:1777–1793.
[89] Grant CA, Twigg PC, Tobin DJ. Static and dynamic nanomechanical properties of human skin tissue using atomic force microscopy: effect of scarring in the upper dermis. Acta Biomater. 2012;8:4123–4129.
[90] Dolega M, Zurlo G, Le Goff M, et al. Mechanical behavior of multi-cellular spheroids under osmotic compression. J Mech Phys Solids. 2021;147:1–21.
[91] Vyas V, Solomon M, D'Souza GGM, et al. Nanomechanical analysis of extracellular matrix and cells in multicellular spheroids. Cell Mol Bioeng. 2019;12:203–214.
[92] Jaiswal D, Cowley N, Bian Z, et al. Stiffness analysis of 3D spheroids using microtweezers. PLoS ONE. 2017;12:1–21.
[93] Hochmuth RM. Micropipette aspiration of living cells. J Biomech. 2000;33:15–22.
[94] Shojaei-Baghini E, Zheng Y, Sun Y. Automated micropipette aspiration of single cells. Ann Biomed Eng. 2013;41:1208–1216.
[95] Schiffhauer ES, Luo T, Mohan K, et al. Mechanoaccumulative elements of the mammalian actin cytoskeleton. Curr Biol. 2016;26:1473–1479.
[96] Maître JL, Niwayama R, Turlier H, et al. Pulsatile cell-autonomous contractility drives compaction in the mouse embryo. Nat Cell Biol. 2015;17:849–855.
[97] Guevorkian K, Colbert M-J, Durth M, et al. Aspiration of biological viscoelastic drops. Phys Rev Lett. 2010;104:1–4.
[98] Guevorkian K, Gonzalez-rodriguez D, Carlier C, et al. Mechanosensitive shivering of model tissues under controlled aspiration. PNAS. 2011;108:13387–13392.
[99] Krishnan R, Park CY, Lin YC, et al. Reinforcement versus fluidization in cytoskeletal mechanoresponsiveness. PLoS ONE. 2009;4:e5486.
[100] Yusheng W, Zanotelli MR, Zhang J, et al. Matrix-driven changes in metabolism support cytoskeletal activity to promote cell migration. Biophys J. 2021;120:1705–1717.
[101] Engler AJ, Sen S, Sweeney HL, et al. Matrix elasticity directs stem cell lineage specification. Cell. 2006;126:677–689.
[102] Zahn JT, Louban I, Jungbauer S, et al. Age-dependent changes in microscale stiffness and mechanoresponses of cells. Small. 2011;7:1480–1487.
[103] Acerbi I, Cassereau L, Dean I, et al., Human breast cancer invasion and aggression correlates with ECM stiffening and immune cell infiltration. Integr Biol U K. 2015;7:1120–1134.
[104] Najafi M, Farhood B, Mortezaee K. Extracellular matrix (ECM) stiffness and degradation as cancer drivers. J Cell Biochem. 2019;120:2782–2790.
[105] Zimberlin JA, McManus JJ, Crosby AJ. Cavitation rheology of the vitreous: mechanical properties of biological tissue. Soft Matter. 2010;6:3632–3635.
[106] Zimberlin JA, Sanabria-Delong N, Tew GN, et al. Cavitation rheology for soft materials. Soft Matter. 2007;3:763–767.
[107] Chaudhuri O, Cooper-White J, Janmey PA, et al. Effects of extracellular matrix viscoelasticity on cellular behaviour. Nature. 2020;584:535–546.

[108] Christoph Mark TJ, Grundy PL, Strissel DB, et al. Collective forces of tumor spheroids in three-dimensional biopolymer networks. eLife. 2020;9:1–22.
[109] Helmlinger G, Netti PA, Lichtenbeld HC, et al. Solid stress inhibits the growth of multicellular tumor spheroids. Nat Biotechnol. 1997;15:778–783.
[110] Taubenberger AV, Girardo S, Träber N, et al. 3D microenvironment stiffness regulates tumor spheroid growth and mechanics via p21 and ROCK. Adv Biosyst. 2019;3:1–16.
[111] Delarue M, Montel F, Vignjevic D, et al. Compressive stress inhibits proliferation in tumor spheroids through a volume limitation. Biophys J. 2014;107:1821–1828.
[112] Mok S, Habyan SA, Ledoux C, et al. Mapping cellular-scale internal mechanics in 3D tissues with thermally responsive hydrogel probes. Nat Commun. 2020;11. DOI:10.1038/s41467-020-18469-7
[113] Dolega ME, Delarue M, Ingremeau F, et al. Cell-like pressure sensors reveal increase of mechanical stress towards the core of multicellular spheroids under compression. Nat Commun. 2017;8. DOI:10.1038/ncomms14056
[114] Tse JR, Engler AJ. Preparation of hydrogel substrates with tunable mechanical properties. Curr Protoc Cell Biol. 2010;47:10.16.1–10.16.16.
[115] Dolega ME, Monnier S, Brunel B, et al. Extra-cellular matrix in multicellular aggregates acts as a pressure sensor controlling cell proliferation and motility. eLife. 2021;10:1–33.
[116] Campàs O, Mammoto T, Hasso S, et al. Quantifying cell-generated mechanical forces within living embryonic tissues. Nat Methods. 2014;11:183–189.
[117] Pei Y, Chen J, Yang L, et al. The effect of pH on the LCST of poly (N-isopropylacrylamide) and poly(N-isopropylacrylamide-co-acrylic acid). J Biomater Sci Polym Ed. 2004;15:585–594.
[118] Morais JM, Papadimitrakopoulos F, Burgess DJ. Biomaterials/tissue interactions: possible solutions to overcome foreign body response. AAPS J. 2010;12:188–196.
[119] Sunyer R, Trepat X, Fredberg JJ, et al. The temperature dependence of cell mechanics measured by atomic force microscopy. Phys Biol. 2009;6:025009.
[120] Valentine MT, Dewalt LE, Ou-Yang HD. Forces on a colloidal particle in a polymer solution: a study using optical tweezers. J Phys Condens Matter. 1996;8:9477–9482.
[121] Bustamante C, Bryant Z, Smith SB. Ten years of tension: single-molecule DNA mechanics. Nature. 2003;421:423–427.
[122] Ashkin A. Optical trapping and manipulation of small neutral particles using lasers. Proc Natl Acad Sci U S A. 1997;94:4853–4860.
[123] Gutsche C, Elmahdy MM, Kegler K, et al. Micro-rheology on (polymer-grafted) colloids using optical tweezers. J Phys Condens Matter. 2011;23:184114.
[124] Han YL, Pegoraro AF, Hui L, et al. Cell swelling, softening and invasion in a three-dimensional breast cancer model. Nat Phys. 2020;16:101–108.
[125] Posy S, Shapiro L, Honig B. Sequence and structural determinants of strand swapping in cadherin domains: do all cadherins bind through the same adhesive interface? J Mol Biol. 2008;378:954–968.
[126] Imamura Y, Itoh M, Maeno Y, et al. Functional domains of alpha-catenin required for the strong state of cadherin-based cell adhesion. J Cell Biol. 1999;144:1311–1322.
[127] Chu YS, Thomas WA, Eder O, et al. Force measurements in E-cadherin-mediated cell doublets reveal rapid adhesion strengthened by actin cytoskeleton remodeling through Rac and Cdc42. J Cell Biol. 2004;167:1183–1194.
[128] Yamada S, Pokutta S, Drees F, et al. Deconstructing the cadherin-catenin-actin complex. Cell. 2005;123:889–901.

[129] Amack JD, Manning ML. Knowing the boundaries: extending the differential adhesion hypothesis in embryonic cell sorting. Science. 2012;338:212–215.
[130] Lecuit T, Lenne P-F. Cell surface mechanics and the control of cell shape, tissue patterns and morphogenesis. Nat Rev Mol Cell Biol. 2007;8:633–644.
[131] Krieg M, Puech P, Käfer J, et al. Tensile forces govern germ-layer organization in zebrafish. Nat Cell Biol. 2008;10:429–436.
[132] Farhadifar R, Jens-christian R, Aigouy B, et al. The influence of cell mechanics, cell-cell interactions, and proliferation on epithelial packing. Curr Biol. 2007;17:2095–2104.
[133] Brodland GW. The differential interfacial tension hypothesis (DITH): a comprehensive theory for the self-rearrangement of embryonic cells and tissues. J Biomech Eng. 2002;124:188–197.
[134] Mertz AF, Banerjee S, Che Y, et al. Scaling of traction forces with the size of cohesive cell colonies. Phys Rev Lett. 2012;108:1–5.
[135] Steve Pawlizak AW, Fritsch SG, Ahrens D, et al. Testing the differential adhesion hypothesis across the epithelial-mesenchymal transition. New J Phys. 2015;17:083049.
[136] Maruthamuthu V, Sabass B, Schwarz US, et al. Cell-ECM traction force modulates endogenous tension at cell-cell contacts. Proc Natl Acad Sci U S A. 2011;108:4708–4713.
[137] Monier B, Pélissier-Monier A, Sanson B. Establishment and maintenance of compartmental boundaries: role of contractile actomyosin barriers. Cell Mol Life Sci. 2011;68:1897–1910.
[138] Laplante C, Nilson LA. Differential expression of the adhesion molecule Echinoid drives epithelial morphogenesis in Drosophila. Development. 2006;133:3255–3264.
[139] Ninomiya H, Robert David EW, Damm FF, et al. Cadherin-dependent differential cell adhesion in xenopus causes cell sorting in vitro but not in the embryo. J Cell Sci. 2012;125:1877–1883.
[140] Canty L, Zarour E, Kashkooli L, et al. Sorting at embryonic boundaries requires high heterotypic interfacial tension. Nat Commun. 2017;8. DOI:10.1038/s41467-017-00146-x
[141] Fagotto F, Winklbauer R, Rohani N. Ephrin-Eph signaling in embryonic tissue separation. Cell Adh Migr. 2014;8:308–326.
[142] Dapeng B, Lopez JH, Schwarz JM, et al. A density-independent rigidity transition in biological tissues. Nat Phys. 2015;11:1074–1079.
[143] Atia L, Dapeng B, Yasha Sharma JA, et al. Geometric constraints during epithelial jamming. Nat Phys. 2018;14:613–620.
[144] Park JA, Kim JH, Dapeng B, et al. Unjamming and cell shape in the asthmatic airway epithelium. Nat Mater. 2015;14:1040–1048.
[145] Dapeng B, Yang X, Cristina Marchetti M, et al. Motility-driven glass and jamming transitions in biological tissues. Phys Rev X. 2016;6:1–13.
[146] Hanahan D, Weinberg RA. Hallmarks of cancer: the next generation. Cell. 2011;144:646–674.
[147] Thiery JP, Acloque H, Huang RYJ, et al. Epithelial-mesenchymal transitions in development and disease. Cell. 2009;139:871–890.
[148] Chao YL, Shepard CR, Wells A. Breast carcinoma cells re-express E-cadherin during mesenchymal to epithelial reverting transition. Mol Cancer. 2010;9:1–18.
[149] Mitchel JA, Das A, O'Sullivan MJ, et al. In primary airway epithelial cells, the unjamming transition is distinct from the epithelial-to-mesenchymal transition. Nat Commun. 2020;11:1–14.

[150] Kim JH, Pegoraro AF, Das A, et al. Unjamming and collective migration in MCF10A breast cancer cell lines. Biochem Biophys Res Commun. 2020;521:706–715.
[151] Friedl P, Locker J, Sahai E, et al. Classifying collective cancer cell invasion. Nat Cell Biol. 2012;14:777–783.
[152] Christiansen JJ, Rajasekaran AK. Reassessing epithelial to mesenchymal transition as a prerequisite for carcinoma invasion and metastasis. Cancer Res. 2006;66:8319–8326.
[153] Padmanaban V, Krol I, Yasir Suhail BM, et al. E-cadherin is required for metastasis in multiple models of breast cancer. Nature. 2019;573:439–444.
[154] Fischer KR, Durrans A, Lee S, et al. Epithelial-to-mesenchymal transition is not required for lung metastasis but contributes to chemoresistance. Nature. 2015;527:472–476.
[155] Huang YL, Shiau C, Cindy W, et al. The architecture of co-culture spheroids regulates tumor invasion within a 3D extracellular matrix. Biophys Rev Lett. 2020;15:131–141.
[156] Yamada KM, Sixt M. Mechanisms of 3D cell migration. Nat Rev Mol Cell Biol. 2019;20:738–752.
[157] Doolin MT, Moriarty RA, Stroka KM. Mechanosensing of mechanical confinement by mesenchymal-like cells. Front Physiol. 2020;11:1–19.
[158] Venturini V, Pezzano F, Castro FC, et al. The nucleus measures shape changes for cellular proprioception to control dynamic cell behavior. Science. 2020;370:eaba2644.
[159] Lomakin AJ, Cattin CJ, Cuvelier D, et al. The nucleus acts as a ruler tailoring cell responses to spatial constraints. Science. 2020;370:eaba2894.
[160] Goncalves IG, Manuel J, Aznar G, et al. Extracellular matrix density regulates the formation of tumour spheroids through cell migration. PLoS Comput Biol. 2021;17:1–22.
[161] Follain G, Herrmann D, Harlepp S, et al. Fluids and their mechanics in tumour transit: shaping metastasis. Nat Rev Cancer. 2020;20:107–124.
[162] Levental KR, Yu H, Kass L, et al. Matrix crosslinking forces tumor progression by enhancing integrin signaling. Cell. 2009;139:891–906.
[163] Huang YL, Yujie M, Cindy W, et al. Tumor spheroids under perfusion within a 3D microfluidic platform reveal critical roles of cell-cell adhesion in tumor invasion. Sci Rep. 2020;10:9648.
[164] Carey SP, Martin KE, Reinhart-King CA. Three-dimensional collagen matrix induces a mechanosensitive invasive epithelial phenotype. Sci Rep. 2017;7:1–14.
[165] Kang W, Ferruzzi J, Spatarelu C-P, et al. Tumor invasion as non-equilibrium phase separation. bioRxiv [Preprint]. 2020; https://doi.org/10.1101/2020.04.28.066845 .
[166] Angela M, Valencia J, Wu PH, et al. Collective cancer cell invasion induced by coordinated contractile stresses. Oncotarget. 2015;6:43438–43451.
[167] Mcevoy E, Han Y, Guo M, et al. Gap junctions amplify spatial variations in cell volume in proliferating solid tumors. Nat Commun. 2020;11:1–11.
[168] Muzhi X, Yicong W, Shroff H, et al. A scheme for 3-dimensional morphological reconstruction and force inference in the early C. Elegans embryo. PLoS ONE. 2018;13:1–20.
[169] Honghan L, Daiki Matsunaga TS, Matsui HA, et al. Wrinkle force microscopy: a new machine learning based approach to predict cell mechanics from images. arXiv:2102.12069 [Preprint]. 2021.
[170] Kidd ME, Shumaker DK, Ridge KM. The role of Vimentin intermediate filaments in the progression of lung cancer. Am J Respir Cell Mol Biol. 2014;50:1–6.
[171] Hoffman BD, Massiera G, Van Citters KM, et al. The consensus mechanics of cultured mammalian cells. Proc Natl Acad Sci U S A. 2006;103:10259–10264.

[172] Desprat N, Guiroy A, Asnacios A. Microplates-based rheometer for a single living cell. Rev Sci Instrum. 2006;77:055111.
[173] Kawai M, Brandt PW. Sinusoidal analysis: a high resolution method for correlating biochemical reactions with physiological processes in activated skeletal muscles of rabbit, frog and crayfish. J Muscle Res Cell Motil. 1980;1:279–303.
[174] Darling EM, Zauscher S, Guilak F. Viscoelastic properties of zonal articular chondrocytes measured by atomic force microscopy. Osteoarthritis Cartilage. 2006;14:571–579.
[175] Aoki T, Ohashi T, Matsumoto T, et al. The pipette aspiration applied to the local stiffness measurement of soft tissues. Ann Biomed Eng. 1997;25:581–587.
[176] Beatrici A, Baptista LS, Granjeiro JM. Measurement uncertainty evaluation of cellular spheroids surface tension in compressing tests using Young-Laplace equation. J Phys Conf Ser. 2018;975:1-7.
[177] Chin MS, Freniere BB, Fakhouri S, et al. Cavitation rheology as a potential method for in vivo assessment of skin biomechanics. Plast Reconstr Surg. 2013;131:303e–305e.
[178] Guevorkian K, Maître JL. Micropipette aspiration: a unique tool for exploring cell and tissue mechanics in vivo. Cell Polarity Morphogenesis Methods Cell Biol. 2017;139:187–201.